A Comparative Study of Fatigue Damage Sensing in Aluminum Alloys using Electrical Impedance and Laser Ultrasonic Methods

Lindsey Channels[a], Debejyo Chakraborty[b], Brad Butrym[c], Narayan Kovvali[b], James Spicer[a], Antonia Papandreou-Suppappola[b], Mana Afshari[c], Daniel Inman[c] and Aditi Chattopadhyay[d]

[a]Department of Materials Science and Engineering, Johns Hopkins University, Baltimore, MD
[b]Department of Electrical Engineering, Arizona State University, Tempe, AZ
[c]Department of Mechanical Engineering, Virginia Polytechnic Institute, Blacksburg, VA
[d]Department of Mechanical and Aerospace Engineering, Arizona State University, Tempe, AZ

ABSTRACT

Fatigue damage sensing and measurement in aluminum alloys is critical to estimating the residual useful lifetime of a range of aircraft structural components. In this work, we present electrical impedance and ultrasonic measurements in aluminum alloy 2024 that has been fatigued under high cycle conditions. While ultrasonic measurements can indicate fatigue-induced damage through changes in stiffness, the primary indicator is ultrasonic attenuation. We have used laser ultrasonic methods to investigate changes in ultrasonic attenuation since simultaneous measurement of longitudinal and shear properties provides opportunities to develop classification algorithms that can estimate the degree of damage. Electrical impedance measurements are sensitive to changes in the conductivity and permittivity of materials - both are affected by the microstructural damage processes related to fatigue. By employing spectral analysis of impedance over a range of frequencies, resonance peaks can be identified that directly reflect the damage state in the material. In order to compare the impedance and ultrasonic measurements for samples subjected to tension testing, we use processing and classification tools that are matched to the time-varying spectral nature of the measurements. Specifically, we process the measurements to extract time-frequency features and estimate stochastic variation properties to be used in robust classification algorithms. Results are presented for fatigue damage identification in aluminum lug joint specimens.

1. INTRODUCTION

The choice of sensing modality has always been a primary concern in the design and deployment of structural health monitoring systems. While Lamb wave based fatigue damage detection techniques are used in many applications and perform well on damage at larger length-scales, they are not sensitive to microlevel damage. On the other hand, laser ultrasonics provides highly localized measurements and is capable of revealing fatigue damage at the grain level[1], but is not amenable for *in situ* damage detection problems. Electrical impedance measurements[2] are sensitive to changes in the conductivity and permittivity of the material, both of which are affected by the microstructural damage processes related to fatigue. In this paper we study the responses of laser ultrasonic and electrical impedance measurements from fatigue damage in aluminum lug samples. We present analysis of the ultrasonic data that can be correlated with impedance results in order to integrate the discriminatory information gathered by the two different sensing modalities for effective damage identification. This information is used to develop processing and classification tools that are matched to the time-varying spectral nature of the measurements. Ultrasonic and impedance measurements obtained under various structural conditions (damage classes) are processed to extract time-frequency (TF) features and estimate stochastic variation properties. The results of this analysis are entered into classification algorithms. Some preliminary classification results are presented and the challenges due to sample variability are discussed. Time frequency spectra of impedance measurements are shown as a function of fatigue level, indicating sensitivity to the microscale damage.

Health Monitoring of Structural and Biological Systems 2009, edited by Tribikram Kundu,
Proc. of SPIE Vol. 7295, 72950Q · © 2009 SPIE · CCC code: 0277-786X/09/$18 · doi: 10.1117/12.815980

2. EXPERIMENT

2.1 Sample preparation

Specimens, referred to as lug joints, were fabricated out of 2024-T351 to resemble a common aircraft component, Figure 1(a). Using a collection of 15 lug joints, we fatigued half of the specimens by tension, Figure 1(b), in 20,000 cycle increments at 12 Hz with ultrasonic investigations occurring after each interval until the specimen failed, which typically occurred just over 100,000 cycles. Failure occurred at the marked location in Figure 1(a) where the specimen was most susceptible to the fatigue damage. The remainder of the specimens were fatigued to one specific fatigue level, either 20k, 40k, 60k, 80k, or 100k, to allow examination of damage states in the material using destructive techniques. These studies would include, but are not limited to, imaging techniques such as TEM or SEM, and high frequency (1 GHz) ultrasonic testing.

(a)

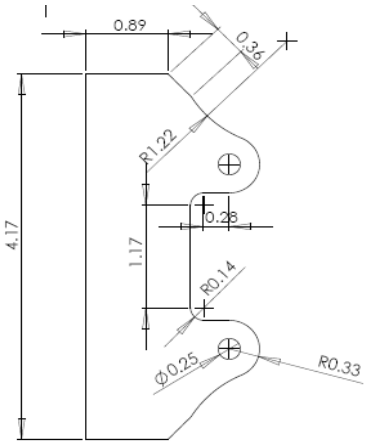

(b)

Figure 1. (a) Specimen in testing apparatus with location of crack formation marked. (b) Schematic of lug joint specimen.

2.2 Data collection procedure

As reported previously by Channels *et al.*[1], the experimental apparatus included a 1064 nm Nd:YAG 10 ns pulsed laser as shown in Figure 2. This was used to generate ultrasound in our specimens with the pulse energy being reduced to 2.4 mJ to avoid material ablation. To detect ultrasonic displacements in the sample, a broadbanded NBS/NIST conical transducer was used. The conical transducer has a frequency response from 20 kHz to 1.5 MHz and significantly increases the signal-to-noise ratio of recorded signals compared to those reported previously.[1]

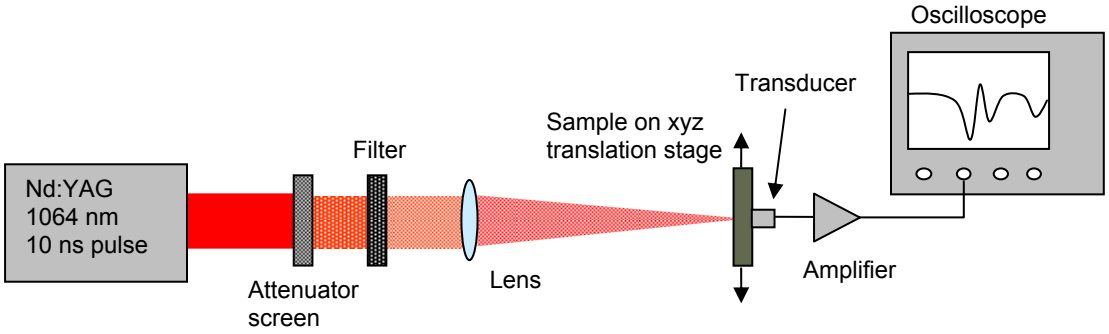

Figure 2. Experimental apparatus used for ultrasonic data acquisition of lug joints

To acquire data, each lug specimen was placed in a mount fixed to a tri-axis micrometer stage. The generation laser was focused to 1.5 mm with a reduction in energy allowing generation of thermoelastic waves without specimen ablation. The transducer was positioned directly on epicenter with the laser on the opposite side of the specimen. Positions of the stage relative to locations concentrated around the area of the lug most susceptible to failure were used to mark data acquisition points. Data were collected at these points on each specimen by averaging 500 waveforms to reduce the noise signature. One location was chosen for reference purposes for each specimen in order to collect data for the signal classification algorithm discussed later in this paper. The location was chosen for its proximity to the region most likely to exhibit failure. Once again, each final waveform represented 500 averaged signals and this measurement was performed 50 to 100 times in the same location in order to train the classifier.

Impedance measurements were carried out on the aluminum lug samples under various fatigue conditions. Several impedance-derived damage indices have been studied in the literature, some of these are presented in Tseng and Wang.[2] In this work, we examine time-varying spectral properties of the impedance measurements in order to verify sensitivity to microlevel damage and correlate them with the information obtained from ultrasonic signals. The frequency-domain impedance measurements from our experiments spanned from 100 Hz to 240 KHz in steps of 20 Hz. The real admittance provides damage-related information while the imaginary part is related to sensor coupling and reflects sensor debonding or other forms of failure.

3. RESULTS AND DISCUSSION

3.1 Preliminary assessment of lug joint ultrasonic and impedance data

Changes in attenuation and wave arrival times can be assessed simply by comparison of individual waveforms. Figure 3(a) displays waveforms generated from the same location on four different lug joints that were in the unfatigued state. The four specimens show fair agreement in wave arrivals and shape, however there is some variation in amplitude. Ultrasonic attenuation is commonly used to monitor microstructural changes in materials, however variations in the attenuations for the unfatigued state present challenges for fatigue monitoring.

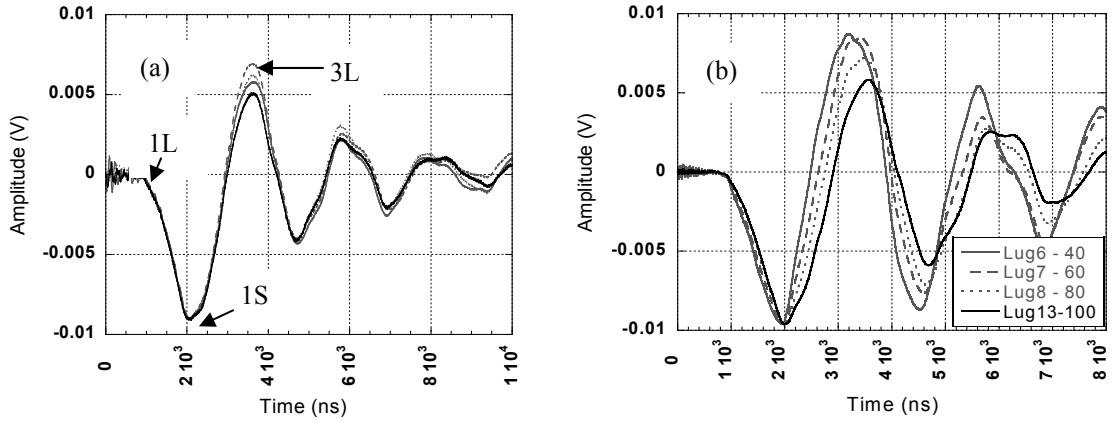

Figure 3. (a) Four unfatigued lug joints (b) Four fatigued lug joints showing greatest amplitude at 40k to lowest amplitude at 100k

Figure 3(b) includes waveforms from four different lug joints fatigued to four different but consecutive fatigue stages ranging from 40,000 to 100,000 fatigue cycles. These waveforms exhibit changes in attenuation as well as variations in the arrival of the reflected longitudinal wave. Changes in attenuation in both Figure 3(a) and 3(b) might be due primarily to initial differences in material microstructure. However it appears that delays in the arrival of the reflected longitudinal wave in Figure 3(b) correlate well with the fatigue state of the material and could be an indicator of microstructural changes in the material.

We have also examined multiple damage states up to 60,000 fatigue cycles in the same lug joint, looking for trends in attenuation and time delay. In addition, impedance measurements performed on the same lug joints should give us better

insight into the physical changes of the microstructure. Using both ultrasonic and impedance measurements could allow us to create a reliable library of fatigue classifications. While casual inspection of our results is interesting, it is clear that we need a more sophisticated classification technique to extract meaningful information as it relates to the fatigue state of the material. Preliminary tests on the ultrasonic and impedance data using time frequency analysis are shown in the following sections.

4. TIME-FREQUENCY ANALYSIS AND PROCESSING

4.1 Matching Pursuit Decomposition and Time-Frequency Studies

Structural data often exhibits time-varying spectral content[1,3-5] and since such behavior is not comprehensively represented in either a time- or frequency-domain-only analysis we employ joint TF analysis. Specifically, the responses from the ultrasonic and impedance measurements are analyzed in the TF plane using a feature extraction procedure based on the matching pursuit decomposition (MPD)[6].

The MPD is an iterative algorithm that attempts to represent a given signal as a weighted linear combination of basis functions (atoms) from a set (dictionary). The atoms are selected from the dictionary based on a maximum projection (best match) criterion, and the representation error (residue) decreases at every MPD iteration. The number of iterations is chosen such that the important signal components are captured, while rejecting any unwanted measurement noise. The MPD representation is adaptive and generally parsimonious, and leads to an efficient characterization of the signal in question in terms of the dictionary atom parameters (features). In this work we use a TF dictionary composed of highly localized Gaussian windowed, time- and frequency-shifted and scaled harmonics with well-know resolution and analytic advantages[3]. The details of the algorithm can be found in[3].

As an example, Figure 5 shows the MPD representation of a preprocessed (see Subsection *Damage Classification*) ultrasonic signal from an unfatigued aluminum lug-joint sample. Note how well the original signal is matched by its MPD representation. Figure 6 shows the residual energy fraction as a function of the MPD iteration number. Exponential convergence is evident and the error is on the order of 10^{-4}. This behavior is typical on the preprocessed ultrasonic signals which were almost noise-free.

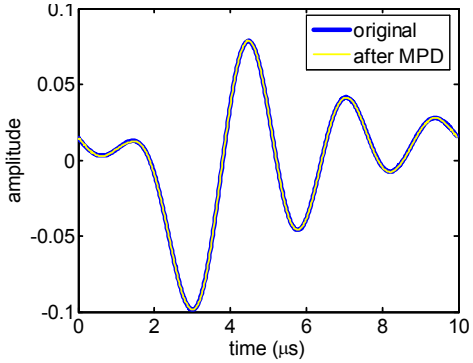

Figure 5. Matching pursuit decomposition representation of an ultrasonic signal from an unfatigued Al lug joint.

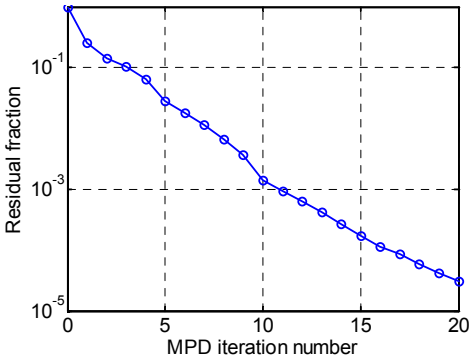

Figure 6. Matching pursuit decomposition convergence for an ultrasonic signal from an unfatigued Al lug joint.

The MPD can be used to compute a joint TF representation (MPD-TFR) of the data[3]. The MPD-TFR is defined as a weighted linear sum of the Wigner distributions (WDs)[7] of the Gaussian MPD atoms and does not suffer from cross-term issues[7]. Figure 7 shows the cross-term free MPD-TFR of the example ultrasonic signal in Figure 5.

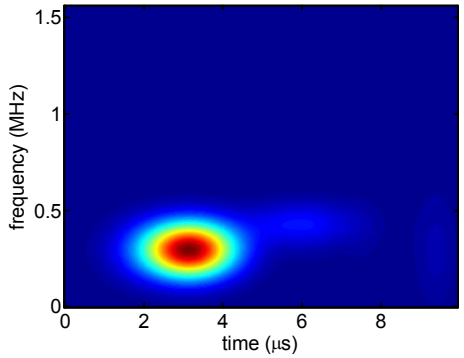

Figure 7. Cross-term free matching pursuit decomposition – time frequency representation of example ultrasonic signal in Figure 5.

In order to ensure that geometry-dependent artifacts do not come into play, analysis is restricted to the first 10 microseconds of the recording of the ultrasonic signals. Some representative preprocessed signals from the various fatigue levels considered are shown in Figure 8 (in both time- and TF domains). The differences between the signals from the various structural conditions are visible as shifts in the arrival times of the longitudinal waves for the fatigued samples. In particular, we observe that the signal shape changes in the presence of damage. The signals from the various fatigued samples look somewhat similar, but are markedly different from that for the unfatigued case. The MPD-TFR reveals some small differences that are not readily visible in the time-plots. Note that each of these signals was measured from a different lug sample and some of the differences in the signatures may be attributed to sample/material variability.

In order to address variability due to differences in microstructure among different samples, the data for each fatigue damage level was collected from several samples. A preliminary dataset contains data from 3 unfatigued lugs, 2 lugs fatigued to 60 kilocycles, 1 to 80 kilocycles, and 2 fatigued until visible cracking to 100 and 230 kilocycles. The signal shown in Figure 8 for the cracked case is a representative signal from the 230 kilocycles fatigue damage class.

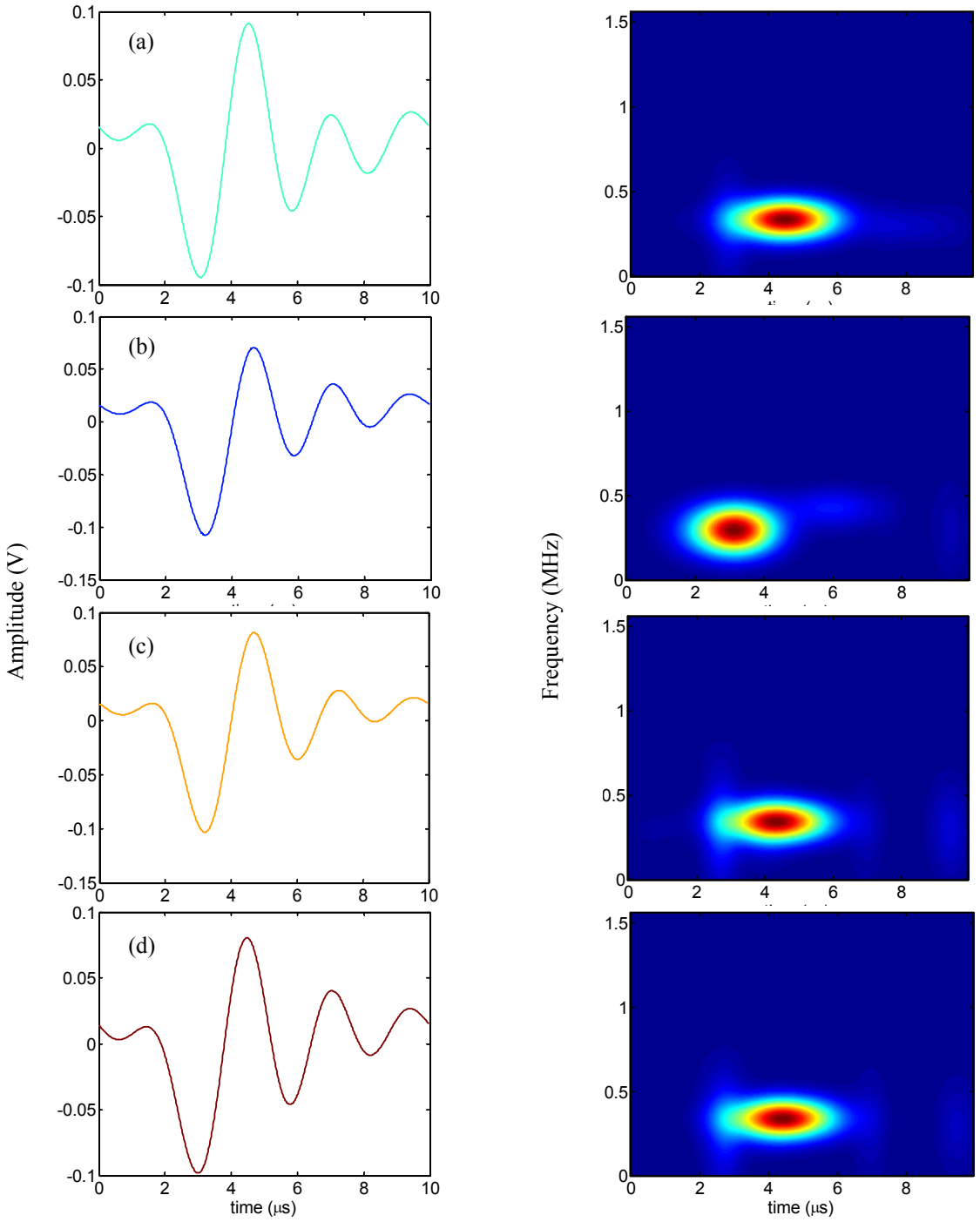

Figure 8. Time-plots and corresponding matching pursuit decomposition - time frequency representations of ultrasonic signals from lug samples fatigued to different levels. (a) Unfatigued (b) Fatigued 60 kilocycles (c) Fatigued 80 kilocycles (d) Visible crack

4.2 Damage Classification

We apply the MPD TF based damage classification approach to the ultrasonic measurements. The collected data was comprised of 154, 102, 50 and 128 signals from each of four structural conditions: unfatigued, 60 kilocycles fatigued, 80

kilocycles fatigued, and visibly cracked, respectively. Each structural condition is defined as a separate damage class. Half of the data from each damage class was used as training data and the other half was used as testing data. As a preprocessing step, all signals were first filtered (to remove out-of-band noise), time aligned with respect to each other (not necessary if they are synchronized at the time of recording), down-sampled, mean-shifted (to offset DC shift), and normalized to unit energy.

Matching pursuit decomposition is then carried out on the signals with a dictionary composed of about 25 million Gaussian atoms. The number of MPD iterations used was 20, corresponding to a residual energy fraction of approximately 0.01 %. The MPD of the signals is then used to compute cross-term free MPD-TFRs for joint TF analysis.

In the MPD TF based damage classification method[3], representative template MPD-TFRs are first defined to characterize the TF structure of the signatures of the signals from each damage class. The training data available from the various damage classes is utilized for this purpose, and the amount of data available dictates the statistical accuracy of the templates. Test data is then classified by identifying the damage class which maximizes the TF space projection between the template MPD-TFR and the test signal.

Two different scenarios were considered in testing the damage classifier. In test scenario I, data from a single lug was used in each damage class. Consequently, the total number of signals available in each damage class was 52, 50, 50, and 76, respectively. Sample variability is not addressed in this scenario. In test scenario II, all of the available data was utilized. Care was taken in defining the training and testing data sets so that an equal share of data was available from every lug in each set.

Preliminary damage classification results are presented in the form of confusion matrices with confidence intervals. The rows of the confusion matrix represent the actual damage classes and the columns the assigned classes. The diagonal entries of the confusion matrix show correct classification probabilities and the off-diagonal entries show misclassification rates. The uncertainty in estimates of these probabilities is quantified here using 95% confidence intervals. As an example, an entry of 0.98 ± 0.02 in row X column Y of a confusion matrix can be interpreted as: "The probability that data actually from class X is classified as belonging to class Y has an expected value of 0.98, and with probability 0.95 or greater, lies between 0.96 and 1". Table 1 shows the classification result for test scenario I. We see that data from all classes except class 4 is classified correctly. The misclassification is attributed to the similarity of the time-frequency signatures of the test data from class 2 to the template TFR of class 4. The reason for this similarity is not very clear at present.

Table 1. Confusion matrix of matching pursuit decomposition time frequency classification results for ultrasonic data (test scenario I).

Damage State	0 kcyc	60 kcyc	80 kcyc	Visible crack
0 kcyc	0.98 ± 0.02	0	0	0
60 kcyc	0	0.98 ± 0.02	0	0
80 kcyc	0	0	0.98 ± 0.02	0
Visible crack	0	0.98 ± 0.02	0	0.02 ± 0.02

The classification results from test scenario II are presented in Table 2. We find that the performance for damage class 4 has improved considerably. This could be due to the fact that sample variability is incorporated in this scenario and the extra data helps to statistically improve the representation of the template MPD-TFRs (for example, the data from class 4 now contains measurements from 2 lugs). However, once again owing to similarities between time-frequency signatures of different damage classes, the data from class 1 is now incorrectly classified to classes 2 and 3.

Table 2. Confusion matrix of matching pursuit decomposition time frequency classification results for ultrasonic data (test scenario II).

Damage State	0 kcyc	60 kcyc	80 kcyc	Visible crack
0 kcyc	0	0.18 ± 0.06	0.82 ± 0.06	0
60 kcyc	0	0.99 ± 0.01	0	0
80 kcyc	0	0	0.98 ± 0.02	0
Visible crack	0	0	0	0.99 ± 0.01

4.3 Impedance Data

Figure 9 shows real admittance data from the aluminum lug joint for each of the fatigue levels considered earlier. The spectral plots show the frequency-domain data as measured and the spectrograms (magnitude Short-Time Fourier Transforms) show the joint TF distributions of the data ('time' in these TF plots is a mathematical concept and does not depict any physical phenomenon). Differences are visible among the measurements from the various damage levels, especially at the higher frequencies near 200-240 kHz. The TF window that lies within 30-50 ms and 50-80 kHz shows some differences between the unfatigued sample and the other damage classes. These examples, however, are from a very limited data set and do not account for variability.

5. CONCLUSIONS

Laser ultrasound is a highly localized microscale (time frequency) sensing technique while impedance measurement provides global damage metrics. We have analyzed joint TF responses of data from ultrasonic and impedance sensing modalities for classifying fatigue damage in aluminum lug joint samples. The joint TF analysis shows discriminatory information between the various structural conditions which is otherwise inaccessible (using time- or frequency-domain analysis alone). Preliminary damage classification results have been presented on ultrasonic data and seem to be promising.

Importantly, the TF studies reveal that for successful structural health monitoring the effects of sample/material variability must be isolated and statistically characterized. A start has already been made in this direction by assimilating data from multiple lug samples for each fatigue level and training the classification algorithm on this data set to learn the nature of the variability. A next step might be to make the statistical characterization of the variability vs. damage explicit, and possibly supplement it with inputs from physics.

While similar comments may hold true for impedance measurements as well, our current data set is comprised of a limited number of signals and more data is needed before statistically meaningful conclusions can be drawn. Note that the required data need not be experimentally obtained; data computed using physically based modeling can also be utilized.

Finally, both sensing methods have been observed to show sensitivity to the microscale fatigue damage considered here. This provides opportunities for using both sensing methods in conjunction to obtain complementary damage information which can be integrated for robust damage identification.

From the information presented we can begin to track changes in the microstructure, correlating shifts in wave arrival with the fatigue state of the material. Monitoring changes in the ultrasonic waveforms will give us insight into when plastic deformation occurs in the material. By performing imaging techniques such as scanning or transmission electron microscopy we hope to identify what initiates this deformation. We are now in pursuit of an explanation of what occurs

at the crack tip, how dislocation pileups cause changes in the stress field, and how monitoring these parameters can lead us to early detection of microcrack formation.

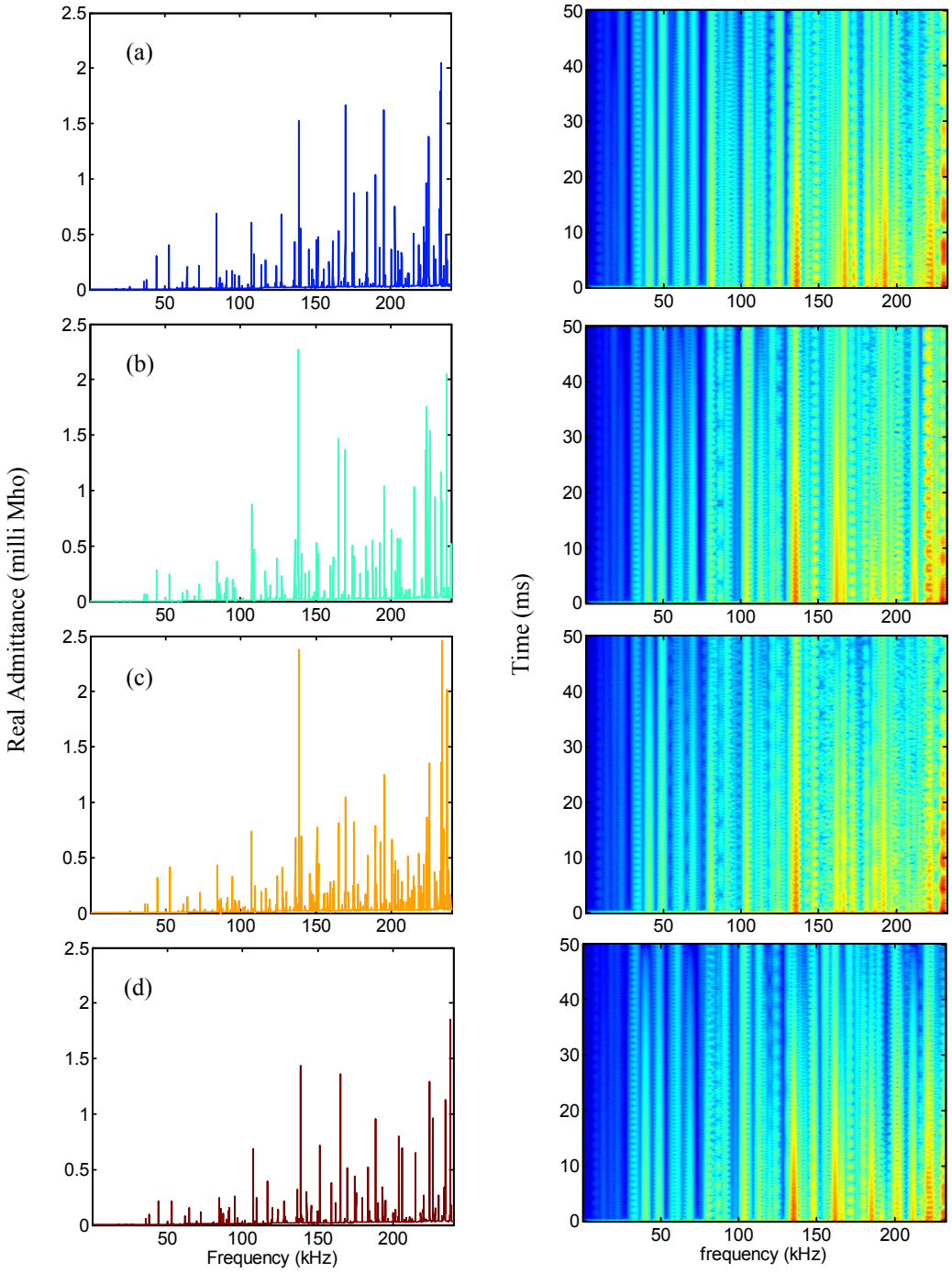

Figure 9. Spectral-plots and their corresponding spectrograms of real admittance data from lug samples fatigued to different levels. (a) Unfatigued (b) Fatigued 60 kilocycles (c) Fatigued 80 kilocycles (d) Visible crack

ACKNOWLEDGEMENTS

Funding for this research was provided by the MURI Program, Air Force Office of Scientific Research, grant number: FA9550-06-1-0309; Technical Monitor, Dr. Victor Giurgiutiu. We would also like to acknowledge Dr. Michael Rooney at the Johns Hopkins Applied Physics Laboratory for use of his expertise and mechanical testing equipment.

REFERENCES

[1] L. Channels, D. Chakraborty, D. Simon, N. Kovvali, J. Spicer, A. Papandreou-Suppappola, D. Cochran, P. Peralta, and A. Chattopadhyay, "Ultrasonic sensing and time-frequency analysis for detecting plastic deformation in an aluminum plate", *Proc. of SPIE*, **6926**, pp. 69260P, 2008.
[2] K. K. Tseng and L. Wang, "Impedance-Based Method for Nondestructive Damage Identification", *Journal of Engineering Mechanics*, **131**, pp. 58-64, 2005.
[3] D. Chakraborty, N. Kovvali, J. Wei, A. Papandreou-Suppappola, D. Cochran, and A. Chattopadhyay, "Damage Classification Structural Health Monitoring in Bolted Structures Using Time-Frequency Techniques", *Journal of Intelligent Material Systems and Structures*, special issue on Structural Health Monitoring, to appear.
[4] W. Zhou, N. Kovvali, A. Papandreou-Suppappola, D. Cochran, A. Chattopadhyay, and W. Reynolds, "Classification of damage in composite structures using hidden Markov models for integrated vehicle health management," *Journal of Intelligent Material Systems and Structures*, special issue on Structural Health Monitoring, to appear.
[5] D. Chakraborty, W. Zhou, D. Simon, N. Kovvali, A. Papandreou-Suppappola, D. Cochran, and A. Chattopadhyay, "Time-frequency methods for structural health monitoring", *Sensor, Signal, and Information Processing Workshop*, Sedona, Arizona, 2008.
[6] S. G. Mallat and Z. Zhang, "Matching pursuits with time-frequency dictionaries," *IEEE Transactions on Signal Processing*, vol. 41, pp. 3397–3415, 1993.
[7] A. Papandreou-Suppappola, Ed., *Applications in Time-Frequency Signal Processing*. Florida: CRC Press, 2002.